



Preparation and characterization of cellulose triacetate polymer inclusion membrane blended with acetylated kraft lignin: effect of AKL and application to the copper(II) extraction from acidic media

Sana Ncib^{a,b}, Afef Barhoumi^a, Wided Bouguerra^c, Christian Larchet^b, Lasâad Dammak^{b,*}, Béchir Hamrouni^c, Elimem Elaloui^a

^aU.R. Matériaux, Environnement et Energie (ME2) (UR 14 ES26), Département de Chimie, Faculté des Sciences de Gafsa-University Gafsa, Campus universitaire Sidi Ahmed Zarroug, 2112 Gafsa, Tunisia, emails: sana_ncib@yahoo.fr (S. Ncib), barhoumiafefe@yahoo.fr (A. Barhoumi), limem_aloui@yahoo.fr (E. Elaloui)

^bInstitut de Chimie et des Matériaux Paris-Est (ICMPE), UMR 7182 CNRS, Université Paris-Est Créteil, 2 Rue Henri Dunant, 94320 Thiais, France, emails: dammak@u-pec.fr (L. Dammak), larchet@u-pec.fr (C. Larchet)

^cU.R. Traitement et dessalement des eaux, Département de Chimie, Faculté des Sciences de Tunis, 2092 Manar II, Tunisia, emails: bg_wided@yahoo.fr (W. Bouguerra), bechir.hamrouni@fst.utm.tn (B. Hamrouni)

Received 6 July 2017; Accepted 14 January 2018

ABSTRACT

In the present work, we analyze the transport properties of a novel polymer inclusion membrane (PIM) containing cellulose triacetate as polymer matrix, acetylated kraft lignin (AKL) as a filler and di-(2-ethylhexyl)phosphoric acid (D2EHPA) as an organic carrier, without addition of supplementary plasticizers. The PIM is characterized by several techniques, to obtain information on their composition and morphology, namely Fourier transform infrared spectroscopy and scanning electron microscopy. Measurements of the contact angle and the tensile strength are realized to have information on hydrophobicity and mechanical properties of the PIM. We have shown that D2EHPA is uniformly dispersed in the polymer matrix. The mechanical properties are considerably improved through the incorporation of the optimal content of 15 wt% of AKL. This last reactant makes membrane surface more hydrophobic and can be used in purification processes of some acidic effluents from chemical industries. As an application, the transport of copper ions from acidic solution through the novel PIM has been investigated. D2EHPA concentration varied from 0 to 40 wt% and we found out that transport of copper(II) increased with the carrier concentration up to 40 wt%. The effect of AKL in membrane composition is studied by using PIM containing 15 wt% of AKL. The incorporation of AKL does not induce significant increase of the initial flux; nevertheless, the novel PIM has a better stability especially in acidic media.

Keywords: Polymer inclusion membranes; Cellulose triacetate; Lignin; D2EHPA; Copper extraction

1. Introduction

Mining activities have huge impact on the environment by generating large amounts of wastewater. Polluted water contains heavy metals of elevated concentration. Copper represents a highly toxic and bioaccumable heavy metal.

A number of technologies, that is, chemical precipitation [1], adsorption [2], ion exchange [3], membrane processes and solvent extraction [4] are available for the separation of this element. The major drawback of these techniques is the requirement of large amount of toxic solvents, production of secondary sludge, high cost, etc.

The polymer inclusion membranes (PIMs) offer high selectivity, low extractant consumption, lower operation costs and operational simplicity [5]. Recently, the PIM systems

* Corresponding author.

have been used as substitute to solvent extraction technique. PIMs are formed by casting a mixture of base polymeric support, plasticizer and ion carrier in volatile solvent such as tetrahydrofuran and methylene chloride, and followed by the slow evaporation of the solvent [6]. The carrier is essentially a complex agent, responsible for binding with the species of interest and transporting it across the PIM. The PIM technology has been efficiently used for both metal ions [5,7,8] and organic molecules extraction [1,9]. Several carriers are studied to improve metal transport efficiency such as tributyl phosphate, alamine 336, tri-*n*-octylphosphine oxide and di-(2-ethylhexyl)phosphoric acid (D2EHPA) [10–13].

The use of a suitable carrier immobilized within the polymer matrix results in a high selectivity of these membranes. Therefore, PIMs stability, chemical resistance and mechanical strength increase compared with supported liquid membranes in which an extractant is dissolved in a diluents. This solution fills the pores of a hydrophobic microporous polymeric membrane [14,15].

The choice of different PIMs constituents depends on both their compatibility to form homogeneous membranes and the nature of the treated solutions. Poly(vinyl chloride) (PVC), polyvinylidene difluoride (PVDF) and cellulose triacetate (CTA) are frequently used as base polymers to form a thin, flexible and stable PIMs. Many studies have reported that PVC and PVDF are more stable because of their better mechanical strength and chemical resistance [6]. In spite of its abundance, the compatibility with many commercial extractants, plasticizers and low cost CTA has several disadvantages namely low mechanical strength, poor resistance to oxidation and hydrolysis in strongly acidic and alkaline solutions [16,17].

Several studies have been conducted to overcome the limitations of CTA by developing mixed matrix-composite membranes. These materials are obtained when using two interpenetrated components: polymer and filler [18]. Wu et al. [19] have demonstrated that the use of biopolymers such as starch and lignin, as fillers of cellulose derivate, is advantageous thanks to its ecofriendly and renewable nature. Compared with inorganic fillers, natural fillers present some well-known advantages such as lower density and price. They are biodegradable, renewable, and their mechanical properties can be comparable with those of inorganic fillers [20].

Lignin, as the second most abundant biopolymeric material in the world after the cellulose, could be used as biofiller and incorporated in acetylated cellulose for the production of composite membranes [21,22]. Lignin's composite has good mechanical properties and a less susceptibility to microbial attack resulting in biofouling [19,23]. Manjarrez Nevarez et al. [24] have chemically modified the lignin by acetylation in order to both change the lignin solubility and increase the interaction with the polymer matrix [22]. Membranes mechanical properties are related to a good particle dispersion of the filler and the carrier as well as to its incorporation into the polymeric matrix.

Considering that the plasticizers used in PIMs preparation are expensive chemicals, the novel PIMs studied in this work are significantly cheaper compared with the plasticized ones as carrier could act as the plasticizer [25,26]. D2EHPA is a highly effective extractant used for the extraction of metal ions. D2EHPA was reported to be an efficient carrier for uranium,

Ni(II), Cd(II), Pb(II) and Cu(II) extraction [10–13]. Advantages of D2EHPA are mainly its chemical stability, high extraction capacity and low solubility in aqueous solutions. Hence, in our study, D2EHPA was selected as extractant-plasticizer [7].

This paper reports on the preparation of a biocomposite inclusion membrane using CTA as a matrix polymer and acetylated lignin as a filler, without addition of a plasticizer. The selectivity of these membranes is modified by the carrier incorporation (D2EHPA). The effects of acetylated lignin on the properties of the resultant membrane are evaluated and analyzed. The resultant PIM is used to extract Cu(II) from acidic solution. The long time behavior of PIMs is also studied.

2. Experimental

2.1. Chemicals

CTA and lignin kraft (KL; product number 370959) provided by Sigma-Aldrich (USA) were used as membrane components to prepare PIMs. D2EHPA (Aldrich 97%) was used as a carrier and as a plasticizer. Methylene chloride (99.9%) was acquired from Sharlab S.L. (Spain) and used without further purification as the solvent. Pyridine, hydrochloric acid and acetic anhydride were of analytical reagent grade and used as-received.

2.2. Lignin acetylation

Lignin used in this work was acetylated with acetic anhydride in the presence of pyridine as a catalyst, leading to acetylated kraft lignin (AKL).

Briefly, the lignin was dried for 24 h at 40°C and acetylated with acetic anhydride/pyridine (1:1, v/v). The mixtures were stirred vigorously at room temperature for 24 h in 250 cm³ Erlenmeyer. After 24 h, the modified lignin was precipitated with hydrochloric acid 10³ mol m⁻³ and stirred for additional laps of 10 min. The solution was filtrated with a vacuum pump and the obtained residue was washed with deionized water. Acetic acid and pyridine removal from the sample was achieved by repeated rinsing in deionized water. The precipitate was dried under vacuum at 40°C for 24 h [27].

2.3. Lignin analysis

2.3.1. Fourier transform infrared spectroscopy

Attenuated total reflectance-Fourier transform infrared (ATR-FTIR) spectra were recorded with a Bruker FTIR spectrometer model Tensor 27 equipped with an ATR crystal. A total of 32 scans were accumulated in transmission mode with a resolution of 2 cm⁻¹.

2.3.2. Nuclear magnetic resonance

All the experiments were recorded on a Bruker Ultrashield Plus 400 spectrometer at 200 MHz, using sample tubes of 5 mm outer diameter at 21°C. Raw and acetylated lignin samples (10 µg) were dissolved in 0.6 cm³ of deuterated chloroform and ¹H NMR spectra were recorded. The measured chemical shifts, expressed in parts per million (ppm), were compared with tabulated values.

2.3.3. Thermal analysis

The thermal properties were evaluated using thermogravimetric analysis (TGA). The TGA was carried out using a Setsys Evolution 16 from SETARAM, thermal analysis instrument. A sample of 5 mg of lignin was dried at 100°C for 30 min to remove moisture. The TGA scan was achieved while heating it from 30°C to 800°C at a rate of 20°C min⁻¹ under nitrogen atmosphere.

2.4. Membrane preparation

The membranes were prepared by solution casting using CH₂Cl₂ (Sigma-Aldrich) as solvent. The determined quantities of CTA and acetylated lignin were separately dissolved into methylene chloride and stirred at room temperature (25°C) for 4 h.

Solutions were then mixed to obtain a casting one. The carrier (D2EHPA) was added to the casting solution under continuous magnetic stirring until homogeneous solution was obtained. The solution was then uniformly spread over an 8.0 cm diameter Petri dish, and covered to assure a slow evaporation of the solvent for 24 h. Then, the obtained membrane was carefully peeled off from the glass dishes, dried and stored in dry conditions at room temperature [28].

2.5. Membrane characterization

2.5.1. Membrane thickness

The thickness of films was determined using a digital micrometer KÄFER by measuring 10 different locations of the membrane. The average value was reported with their accuracy.

2.5.2. Fourier transform infrared spectroscopy

Measurements were performed with a Bruker FTIR spectrometer model Tensor 27 in transmission mode, in the range of 400–4,000 cm⁻¹.

2.5.3. Scanning electron microscopy

Information regarding membrane morphology was obtained by scanning electron microscopy (SEM). Images were recorded with an electron microscope manufactured by Carl Zeiss (Germany) equipped with EDX analyzer.

2.5.4. Contact angle

The contact angle between a pure water drop and the membrane surface was performed using an FM 40 Easy drop (KRÜSS, Germany). The sessile drop technique was used to determine the membrane external hydrophobicity.

2.5.5. Mechanical properties

In order to evaluate the mechanical properties of membranes, the tensile strength and elongation-at-break of membranes were measured by tensile tester INSTRON model 5965L2806. The dried membranes were snipped into a shape with a width of 0.002 m and a total length of 0.012 m.

The stress–strain curves were developed by the instrument software and then the tensile modulus was calculated from the slope of the initial portion of the stress–strain curves. All the samples of membranes were measured at an ambient temperature with a stretching speed of 33.4 μm s⁻¹.

2.5.6. Transport experiments

The transport experiments were carried out in a two-compartment permeation cell made of Teflon with a maximum capacity of 100 cm³. The membrane separates the feed solution consisted of 2.5 mol m⁻³ Cu(II) at pH = 4.5 adjusted with nitric acid from the receiving solution containing HNO₃ 5 × 10⁻⁴ mol m⁻³ solution. Both aqueous feed and stripping solutions were magnetically stirred at 700 rpm at room temperature (25°C). The active surface area of the membrane was 7.10 cm². 0.2 cm³ samples were collected, from feed and receiving solutions, at regular time intervals during the 24 h duration of the experiment. Cu(II) concentrations were determined by atomic absorption spectrophotometer (Analytic Jenna model NoVAA400) for each sample.

3. Results and discussion

3.1. Acetylated lignin characterization

Lignin was chemically modified by the acetylation of its hydroxyl groups in order to enhance the interaction with CTA in the composite. FTIR, nuclear magnetic resonance (NMR) and TGA were used to characterize the acetylation reaction.

3.1.1. ATR-FTIR spectra

Lignin was chemically modified by acetylation in order to change its solubility and increase the interaction with CTA. In order to confirm the lignin acetylation reaction, the FTIR spectra of acetylated and raw lignin were recorded and the results are shown in Fig. 1. The peaks at 1,596, 1,513 and 1,422 cm⁻¹ are related to the aromatic skeletal vibrations and ring breathing with C–O stretching in lignin. The peak at 1,700 cm⁻¹ is attributed to the carbonyl groups [18,29]. The peak at 2,925 cm⁻¹ can be assigned to C–H stretching in aromatic methoxyl groups and in methyl and methylene groups [30].

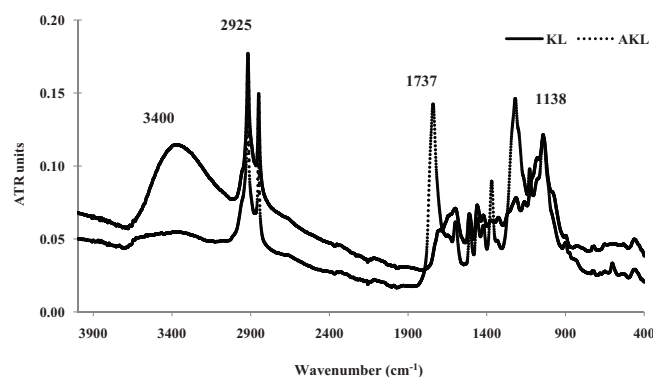


Fig. 1. FTIR-ATR spectra of raw (KL) and acetylated kraft lignin (AKL).

As shown in Fig. 1, the acetylation of lignin resulted in the intensification of the peak between 1,745 and 1,712 cm^{-1} due to the new carbonyl groups linked to the lignin as carboxyl or ester. The carbonyl bonds in esters result in peaks at 1,737 cm^{-1} and a C–O stretching band at 1,138 cm^{-1} .

In addition, the lignin exhibited a wideband around 3,400 cm^{-1} , which is attributed to the stretching of hydroxyl groups in phenolic structures. Acetylation resulted in the decrease of the hydroxyl groups [31].

3.1.2. ^1H NMR spectra

NMR spectra of raw and acetylated lignin are shown in Fig. 2. Methoxy protons ($-\text{OCH}_3$) give an intense signal centered at 4 ppm, which does not vary during the acetylation. Acetylated lignin gives signals from acetate groups at $\delta = 2.1$ ppm (aliphatic acetate) and $\delta = 2.3$ ppm (aromatic acetate) [32,33]. Manjarrez Nevárez et al. [18] have reported that protons of methoxy groups $-\text{OCH}_3$ accord a signal at 3.8 ppm both in unacetylated and acetylated lignin. However, the acetylation increases proton signals assigned to the phenolic and aliphatic acetate groups at $\delta = 2.3$ and 2.1 ppm, respectively.

3.1.3. Thermal analysis

Due to its thermal stability, lignin has an antioxidant property, which opposed oxidative degradation of CTA in lignin-CTA composite. TGA was used to characterize acetylated lignin and verify its thermal stability.

TGA curves obtained for unmodified and acetylated lignin are presented in Fig. 3. As can be seen, the initial degradation of acetylated lignin temperature is marked higher than unmodified lignin with values of 200°C and 180°C, respectively [34]. Degradation of acetylated lignin starts due to the rupture of ester groups [30].

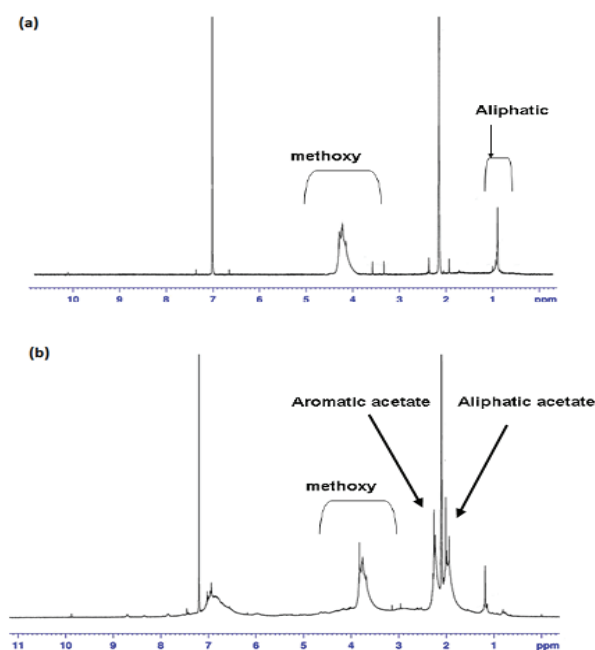


Fig. 2. ^1H NMR spectra of raw (a) and acetylated kraft lignin (b).

At a lower temperature ($<100^\circ\text{C}$), lignin had a small weight loss due to gradual evaporation of moisture; however, acetylated lignin did not show any weight loss.

The weight loss between 300°C and 400°C is attributed to material decomposition of interunits linkage (release of phenolics monomers) [35]. The acetylated lignin also tends to give a higher residue than untreated lignin. The amount of char residue at 800°C was found to be 72% and 56% for AKL and KL, respectively.

3.2. PIMs characterization

3.2.1. Membrane preparation and thickness

The prepared membranes containing 15 and 40 wt% of AKL and D2EHPA, respectively, appear as homogeneous and flexible, while those containing more than 40 wt% of D2EHPA were less mechanically stable. Membranes containing more than 15 wt% of AKL were breakable. As shown in Table 1, for the same total weight of the PIMs initial solution, we observe that the inclusion of D2EHPA into CTA/AKL membrane induced its thickness increase (from 31 to 45 μm). This latter roughly parallels that of carrier molecular weight. The obtained result is in accordance with those obtained in other previous studies [10,36].

3.2.2. ATR-FTIR spectra

The infrared spectroscopy was used to determine the membrane composition and the type of the interactions established between their components.

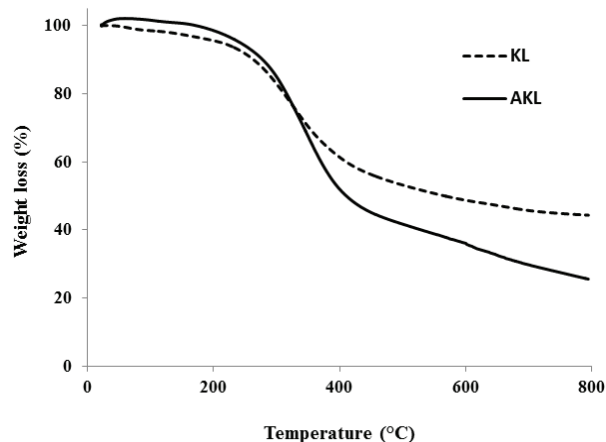


Fig. 3. TGA curves of raw (KL) and acetylated kraft lignin (AKL).

Table 1
Thickness and contact angle for CTA, CTA/AKL and CTA/AKL/D2EHPA membranes

Membrane	D2EHPA (wt%)	Thickness (μm)	Contact angle ($^\circ$)
CTA	0	21 \pm 1	46.8
CTA + AKL	0	31 \pm 2	76.6
CTA + AKL + D2EHPA	20	40 \pm 2	72.8
CTA + AKL + D2EHPA	40	45 \pm 4	62.6

Fig. 4 presents the FTIR spectrum of CTA/AKL/D2EHPA membrane. The peak at $1,735\text{ cm}^{-1}$ is attributed to stretching vibrations of the carbonyl group. The bands at $1,230$ and $1,020\text{ cm}^{-1}$ can be attributed to the stretching modes of C–O single bonds. The wide band detected in the $3,600\text{--}3,100\text{ cm}^{-1}$ region is attributed to the O–H bonds stretching modes [10,37].

Table 2 presents the characteristic groups of D2EHPA: P–O–C and P–O–H showed an intense band at $1,020\text{ cm}^{-1}$, and P=O stretch frequency was observed at $1,230\text{ cm}^{-1}$. The alkyl groups have been assigned at $2,925\text{ cm}^{-1}$ (stretching vibration), $1,460$ and $1,375\text{ cm}^{-1}$ ($-\text{CH}_2$ deformation) [37].

The obtained results showed that, in addition to the acetylated lignin and the carrier molecules, all peaks in the spectrum of the CTA membrane are present in the modified membranes spectra. This indicates that these compounds did not form any new covalent interactions, but only secondary interactions such as hydrogen bonding or electrostatic interactions. This result is in accordance with those proposed by Bayou et al. [10] as well as with observations made by Yildiz et al. [11].

3.2.3. Scanning electron microscopy

Fig. 5 shows SEM micrographs of CTA membranes incorporating KL and AKL. The membrane made from CTA and KL showed many surface defects. However, the membrane made from CTA and AKL (Fig. 5(b)) formed homogeneous films with a smooth surface. This result shows both a good uniformity and adhesion between the polymer matrix and the filler particles. As reported [24], the obtained results showed that the acetylation increased the chain length and

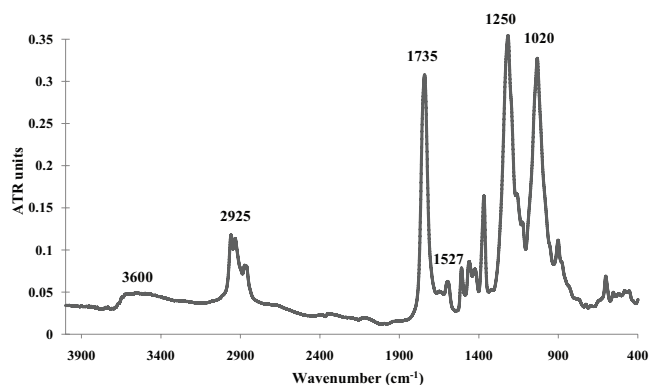


Fig. 4. FTIR spectrum of CTA/AKL/D2EHPA PIM.

Table 2
Identified FTIR-ATR absorption bands in the membrane samples

Peak value (cm^{-1})	Groups
3,600	For CTA O–H
2,925	For AKL C–H (methyl and methylene groups)
1,735	For CTA and AKL C=O
1,527	For CTA COO ⁻
1,230	For D2EHPA P=O
1,020	For D2EHPA P–O–C and P–O–H

the dispersion of modified lignin in CTA. The cross-section image presented in Fig. 5(c) shows that membrane constituted by CTA and AKL presents a microporous structure.

On the other hand, the SEM images in Fig. 6 reveal that the presence of 40 wt% D2EHPA made the membrane surface quite rough (Fig. 6(a)). The cross-section image (Fig. 6(b)) shows that similar carrier distribution is observed. The carrier/plasticizer D2EHPA was entangled in the pores of the polymer making a uniform dense structure with no apparent porosity. This result reinforces the idea that at high D2EHPA

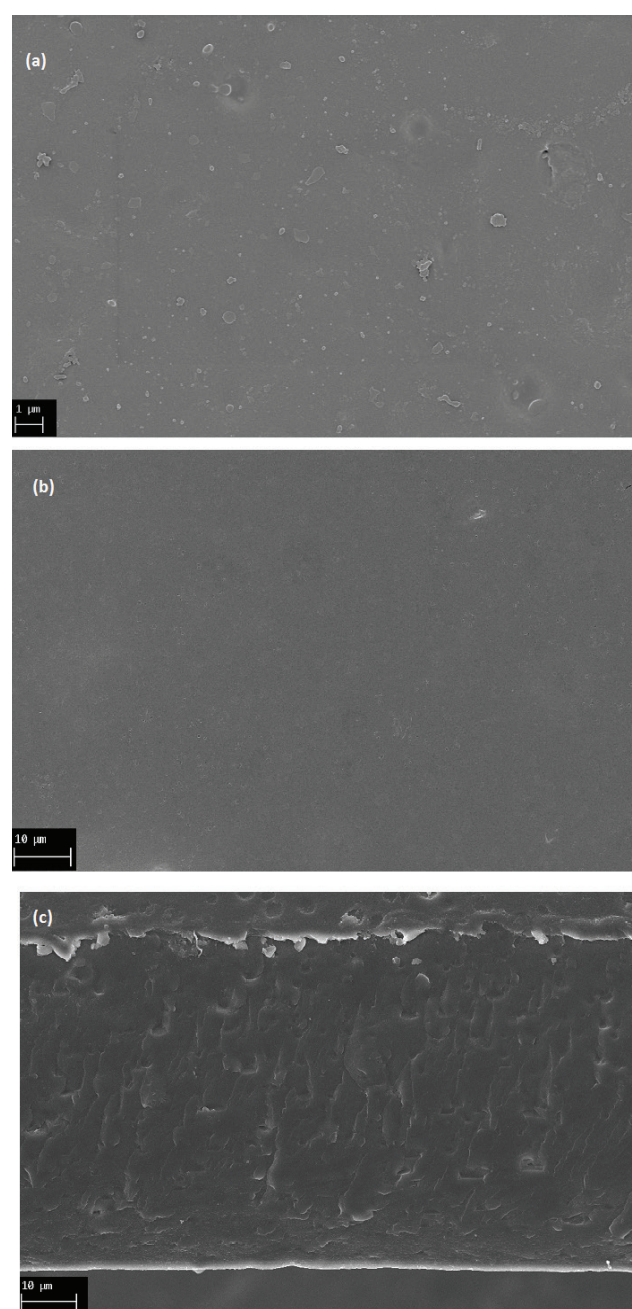


Fig. 5. SEM images of (a) surface of CTA/KL membrane, (b) surface of CTA/AKL membrane and (c) cross-section of CTA/AKL membrane.

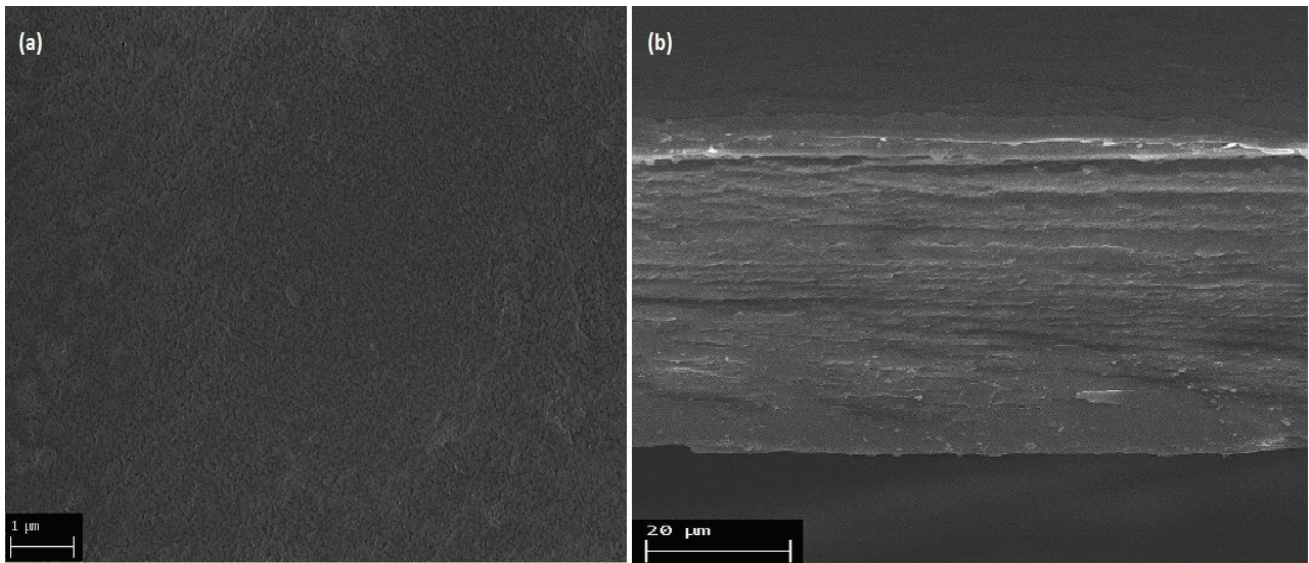


Fig. 6. SEM images of (a) surface of CTA/AKL/D2EHPA membrane and (b) cross-section of CTA/AKL/D2EHPA membrane.

concentrations (ranging from 40 to 50 wt%), the carrier creates liquid pathways which assure the transport process by such PIMs. Similar results have been already presented in literature [28,37,38].

3.2.4. Contact angle

From Table 1, we can conclude that CTA has a hydrophilic character ($\theta = 46.8^\circ$) and after addition of AKL, composite hydrophobicity increased ($\theta = 76.6^\circ$). Similar findings were observed in a previous paper [24].

The addition of the organic carrier decreased the contact angle. For CTA/AKL blank membrane (containing no D2EHPA) and CTA/AKL membrane containing 20 or 40 wt% of D2EHPA, the contact angles decreased from 76.6° to 72.8° and 62.6° , respectively (Table 1). This can be attributed to an adsorption process on the organic carrier molecules at the interface between air and the organic liquid domains, the hydrophilic part of the molecule oriented towards the PIM interface as it would be expected. D2EHPA decreased the resistance against the movement of the water droplet on the membrane surface. These results are in good agreement with the contact angle measurements reported by others in previous works [13,16,39,40].

3.2.5. Mechanical properties

Generally, the addition of the filler is known by improving mechanical properties of the composites [24,30,41]. It was found out that the tensile modulus was increasing with filler loading. Young's or elasticity modulus for each membrane was obtained from the slope of the linear part of the elastic curve at low deformation. In CTA/AKL nanocomposite, Young's modulus increased from 0.87 to 2.11 GPa with 15 wt% modified lignin loading (Fig. 7). The novel membrane showed better mechanical performance.

The tensile strength at break and elongation at break for CTA and acetylated lignin membranes with and without D2EHPA are presented in Fig. 8. D2EHPA amounts are

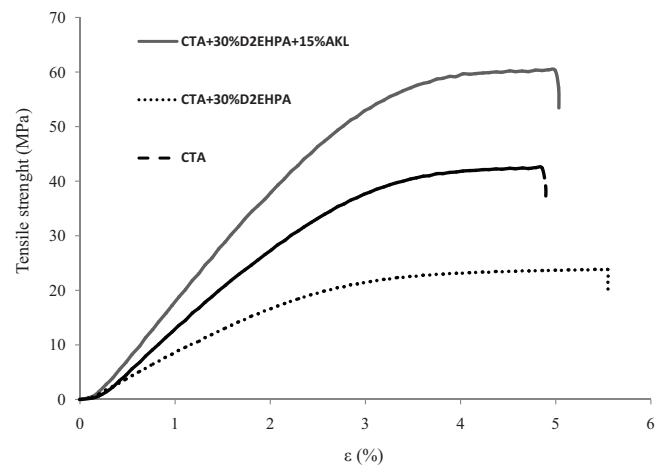


Fig. 7. Tensile strength curves for CTA, CTA/D2EHPA and CTA/D2EHPA/AKL membranes.

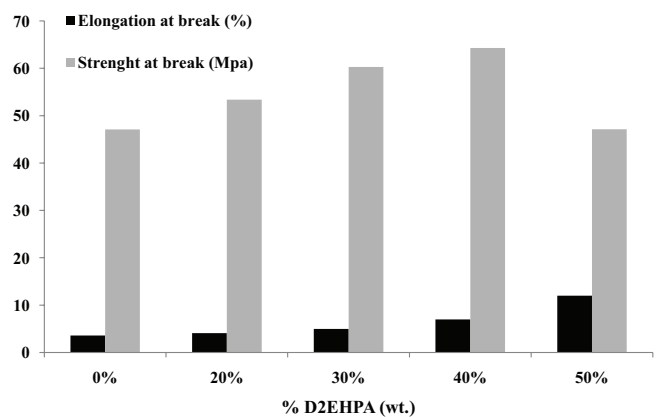


Fig. 8. Mechanical properties of PIMs with CTA, acetylated lignin and different amounts of D2EHPA.

varied from 0 to 50 wt%. It was clear that tensile strength increased gradually as D2EHPA amount increases, which confirm that the used carrier D2EHPA acts as a plasticizer of the CTA–AKL network. This result is in agreement with another work [26]. The tensile strength reaches its maximum for an amount of 40 wt% of D2EHPA. However, it decreased significantly in higher plasticizer level of 50 wt%. In fact, this result confirms that an excessive plasticizer quantity can reduce the membrane mechanical strength.

Results of elongation at break (Fig. 8) show that deformation of the film increases gradually with the level of D2EHPA. This finding could be explained by the corresponding increase of the mobility of CTA molecular chain with the increase of the plasticizer level making the film more flexible [5].

The tensile strength increased from 47 MPa of CTA/AKL membranes (without D2EHPA) to 64 MPa of the optimal membrane (containing 40 wt% of D2EHPA). The elongation-at-break of the optimal membrane composition could reach 11.7%, three times more than 3.6% of the CTA/AKL membranes. The optimum condition, with best mechanical properties, corresponds to 40 wt% of D2EHPA. With this composition, our prepared PIM has better mechanical properties compared with some PIMs described by Vázquez et al. [42].

3.2.6. Influence of membrane characteristics on the copper(II) transport

Copper(II) transport process with D2EHPA was investigated by Kavitha and Palanivelu [13]. The driving force for the mass transfer is an excess of protons in the stripping phase compared with the feed phase. The extraction equilibrium can be described by the following reaction:



where org and aq stand for organic and aqueous solutions, respectively; $(\text{HR})_2$ is a dimeric form of D2EHPA in chloroform. The removal efficiency (E) was calculated according to the following equation [43]:

$$E(\%) = \frac{C_0 - C_t}{C_0} \times 100 \quad (2)$$

where C_0 is the initial metal concentration (mol m^{-3}) in the source solution and C_t is the metal concentration (mol m^{-3}) in the source solution at time t .

3.2.6.1. Comparison of the performance of CTA-AKL-based and CTA-based PIM The effect of AKL as filler on the extraction performance of PIM containing 40 wt% of D2EHPA was conducted using a 2.5 mol m^{-3} Cu^{2+} solution of pH = 4.5. The stripping solution is HNO_3 ($5 \times 10^{-4} \text{ mol m}^{-3}$). From the data reported in Fig. 9, it can be observed that the transport efficiency of copper(II) decreases slightly from 74.4% to 69.4% through CTA-based PIM and the CTA-AKL-based PIM, respectively. The hydrophilic surface of the CTA membrane facilitates the access of extracted solutes to the membrane.

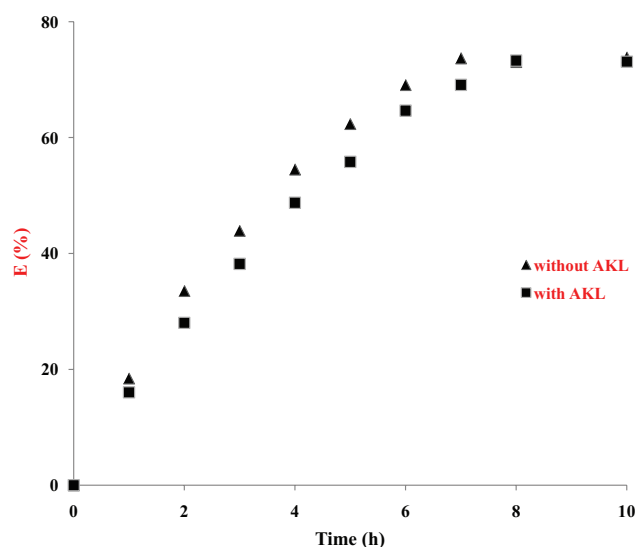


Fig. 9. Amount of Cu(II) transport from feed solution to receiving solution (■) with and (▲) without AKL as filler in CTA-based PIM containing 40 wt% of D2EHPA. Initial Cu^{2+} concentration is 2.5 mol m^{-3} ; feed pH = 4.5; receiving solution is $5 \times 10^{-4} \text{ mol m}^{-3}$ HNO_3 .

However, the addition of AKL makes the surface more hydrophobic and then makes the diffusion of solutes slower. Similar results were obtained in previous works reported that chemical composition of the membrane affects their transport efficiency [44,45].

3.2.6.2. Effect of the organic carrier concentration The ability of D2EHPA in CTA-AKL-based PIM to transport Cu(II) was studied. Here, the feed solution was a 2.5 mol m^{-3} Cu(II), pH = 4.5 adjusted with nitric acid. The stripping solution was a HNO_3 solution ($5 \times 10^{-4} \text{ mol m}^{-3}$). The concentration of D2EHPA was changed in the range of 10–40 wt% in the membrane.

The result of transport experiment using the PIM without carrier showed that in the absence of carrier no transport of copper was detected. This result established that the PIM without carrier served as an effective barrier to ion permeation.

The plots presented in Fig. 10 show that Cu(II) extraction efficiency increases with the rise of the amount of the carrier. A maximum extraction efficiency (74%) was obtained for membranes containing 40% carrier with an equilibrium reached in about 12 h.

Fig. 11 represents the evolution of copper(II) ions concentration in the feed and stripping solutions and in the membrane phase as a function of time using 40 wt% of D2EHPA as carrier in the PIM.

Cu(II) gets transported into the stripping solution with the increase in time. As shown in Fig. 11(b), the Cu(II) amount inside the membrane rises at the beginning to attain a maximum after 1 h of transport and decreases slowly corresponding to the progress of Cu(II) discharge into the stripping phase. This result is comparable with that reported by Kebiche-Senhadjji et al. [38].

From the slope of the tangent obtained when plotting the copper concentration in the stripping phase as a function of time, the initial flux (J_0) can be calculated by the following equation:

$$J_0 = \frac{V}{A} \frac{d[\text{Cu}^{2+}]_R}{dt} \quad (3)$$

where V is the volume of the aqueous stripping solution (m^3), A is the effective exposed surface area of the membrane (m^2) and $[\text{Cu}^{2+}]_R$ is the copper concentration in the stripping solution (mol m^{-3}) as a function of time (s).

As expected, Table 3 showed that the initial flux value increased with the concentration of D2EHPA rise because of both enhanced membrane flexibility and larger amount of extractant. This may be explained by the increase in D2EHPA concentration that would lead to more Cu(II)–D2EHPA complex formation and hence to the increase of its concentration gradient.

By comparing the obtained results to some previously reported works using PIMs containing different carriers for Cu(II) ions transport (Table 4), it can be stated that there is a huge difference in terms of copper flux as one of the most interesting findings in this work.

However, higher initial flux are reported by Tor et al. [39], who studied the competitive transport of Cr(III), Cu(II) and Ni(II) through the PIM with D2EHPA as carrier.

The transport mechanism is the same as proposed by Tor et al. [39]. D2EHPA reacts with Cu ions at the feed phase–membrane interface by ion exchange of protons. The formed complex diffuses across the membrane and the Cu ions are released at the membrane–stripping interface due to the proton higher concentration. This mechanism is known as facilitated transport.

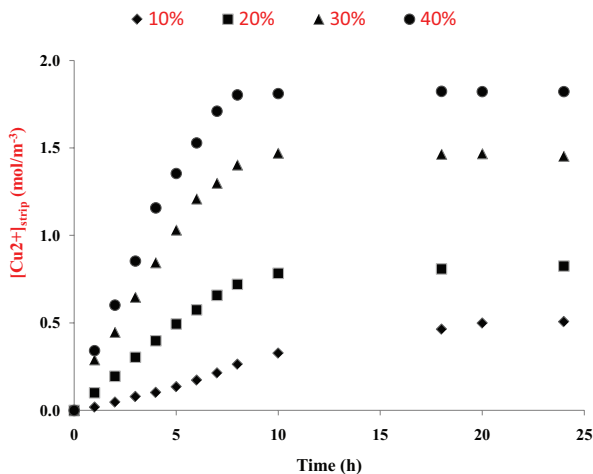


Fig. 10. Copper(II) extraction curves for CTA-AKL-based membranes with different composition of D2EHPA (◆ 10 wt%, ■ 20 wt%, ▲ 30 wt%, ● 40 wt% D2EHPA); initial Cu^{2+} concentration is 2.5 mol m^{-3} ; feed pH = 4.5; receiving solution is $5 \times 10^{-4} \text{ mol m}^{-3} \text{ HNO}_3$.

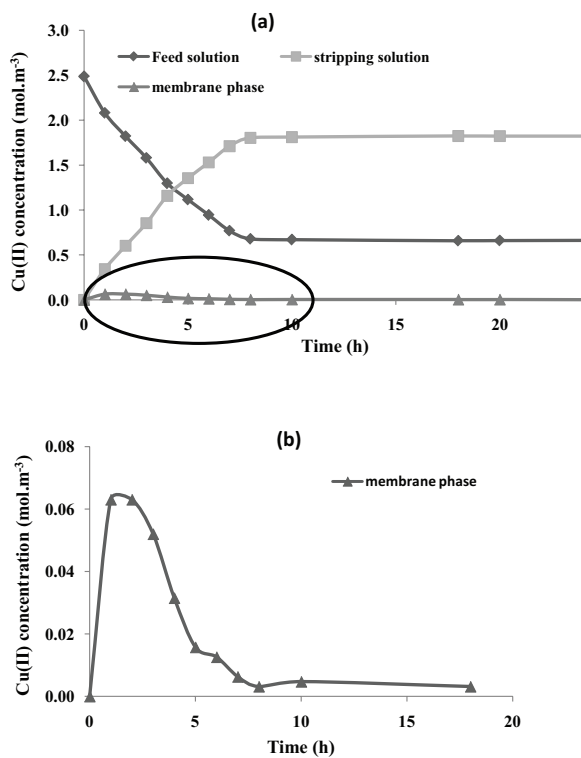


Fig. 11. Concentration profile of Cu(II) in the feed and strip solutions (a) and in the membrane phase (b) as a function of time (initial Cu^{2+} concentration is 2.5 mol m^{-3} ; feed pH = 4.5; receiving solution is $5 \times 10^{-4} \text{ mol m}^{-3} \text{ HNO}_3$. D2EHPA concentration in PIM: 40 wt%).

Table 3
Initial flux J_0 values for CTA-AKL-based PIMs with different D2EHPA concentrations

D2EHPA concentration (wt%)	J_0 ($10^{-5} \text{ mol m}^{-2} \text{ s}^{-1}$)
10	1.3
20	4.3
30	8.7
40	9.2

Initial Cu^{2+} concentration is 2.5 mol m^{-3} ; feed pH = 4.5; receiving solution is $5 \times 10^{-4} \text{ mol m}^{-3} \text{ HNO}_3$.

Table 4
Initial flux of copper using PIMs with different carriers and concentrations

Carrier	Concentration	J_0 ($10^{-5} \text{ mol m}^{-2} \text{ s}^{-1}$)	Reference
Lauric acid	$2.2 \times 10^{-3} \text{ mol m}^{-3}$	0.12	[15]
DB18C6	1.76 mg cm^{-2}	0.28	[46]
TOA	$10^{-3} \text{ mol m}^{-3}$	0.35	[47]
TIOA	$10^{-3} \text{ mol m}^{-3}$	0.63	[47]
D2EHPA	$5 \times 10^{-4} \text{ mol m}^{-3}$	161	[39]
D2EHPA	40 wt%	9.20	This work

TOA, tri-*n*-octylamine; TIOA= triisooctylamine.

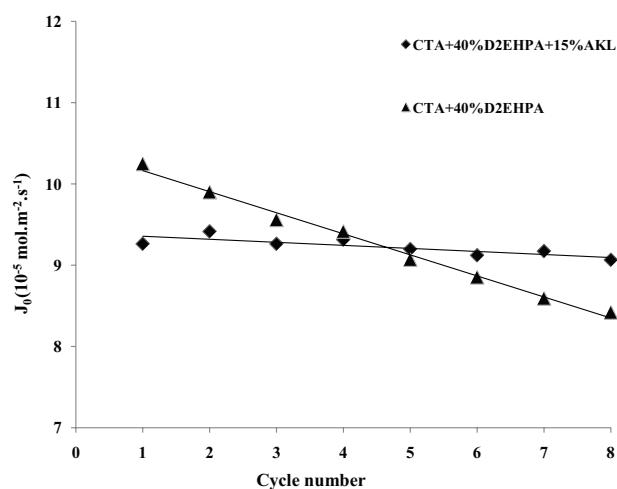


Fig. 12. Stability studies using membrane containing 40 wt% of D2EHPA (♦) with and (▲) without AKL.

3.2.7. Membrane stability

The stability in acidic solution is the most valuable advantage attributed to the novel PIM. In order to test their long-term durability, different experiments were carried out using the same membrane. At each cycle, lasting for 24 h, the two aqueous phases (feed and strip) were replaced.

The evolution of the flux of copper according to the cycle's number is illustrated in Fig. 12 using membrane containing 40 wt% of D2EHPA, with and without AKL. This figure shows that the flux variation with CTA/D2EHPA membrane without AKL shows a gradual decrease of Cu(II) flux. This can be explained by the fact that CTA is prone to hydrolysis under acidic conditions; consequently, the membrane become damaged and missed its properties due to the gradual loss of the membrane's liquid phase [48]. However, the membrane incorporating 15 wt% AKL shows that the flux variation is insignificant. With this novel membrane, our results indicate that no structural weakening was perceived corroborating the good stability for at least eight cycles. The obtained results are in accordance with those obtained in other studies [12,13,49].

4. Conclusion

This paper devoted a new type of biocomposite inclusion membrane. This membrane was prepared by a solution casting using modified lignin as a filler, CTA as a matrix and D2EHPA as a carrier and plasticizer at the same time.

Incorporating AKL in the CTA matrix increased the hydrophobicity, as evidenced by the higher contact angle. The prepared PIMs also showed a good mechanical performance, revealing that AKL stands as a good nanofiller leading to a highest Young's modulus. Both of the tensile strength and elongation-at-break of the blended membranes were enhanced due to the addition of modified lignin and the plasticizer.

The characterization by SEM and FTIR revealed that D2EHPA is well dispersed in the polymer matrix. It constitutes a continuous liquid phase which explains the good PIMs transport properties.

The prepared PIM was used for copper(II) ions transport. Compared with the PIM without AKL, the copper flux slightly decreased. However, this PIM shows a high operational stability and the flux remains constant after a long-term Cu(II) transport. It offers an optimum balance between a lower initial flux and a better stability in acidic media.

The PIM under study does not contain a plasticizer, meant to lower their price and easy manufacturing. It represents important advantages for future uses of the process on a larger scale. It can also be applied in water purification processes, where lignin incorporation would improve the resistance of material to bacteria-induced fouling.

Acknowledgments

This research was funded by the Tunisian Ministry of Higher Education and Scientific Research through the faculty of Science Gabes is gratefully acknowledged. We would like to thank Research Common Services Unit RCSU-Faculty of Sciences Gafsa for their help.

References

- [1] T.A. Kravchenko, L.L. Polyanskiy, V.A. Krysanov, E.S. Zelensky, A.I. Kalinitchev, W.H. Hoell, Chemical precipitation of copper from copper–zinc solutions onto selective sorbents, *Hydrometallurgy*, 95 (2009) 141–144.
- [2] H. Aydın, Y. Bulut, Ç. Yerlikaya, Removal of copper (II) from aqueous solution by adsorption onto low-cost adsorbents, *J. Environ. Manage.*, 87 (2008) 37–45.
- [3] S. Veli, B. Pekey, Removal of copper from aqueous solutions by ion exchange resins, *Fresenius Environ. Bull.*, 13 (2004) 244–250.
- [4] K. Staszak, M. Regel-Rosocka, K. Wieszczycka, P. Burmistrz, Copper(II) sulphate solutions treatment by solvent extraction with Na-Cyanex 272, *Sep. Purif. Technol.*, 85 (2012) 183–192.
- [5] L.D. Nghiem, P. Mornane, I.D. Potter, J.M. Perera, R.W. Cattrall, S.D. Kolev, Extraction and transport of metal ions and small organic compounds using polymer inclusion membranes (PIMs), *J. Membr. Sci.*, 281 (2006) 7–41.
- [6] N. Pereira, A. St John, R.W. Cattrall, J.M. Perera, S.D. Kolev, Influence of the composition of polymer inclusion membranes on their homogeneity and flexibility, *Desalination*, 236 (2009) 327–333.
- [7] C.-V. Gherasim, G. Bourceanu, R.-L. Olariu, C. Arsene, A novel polymer inclusion membrane applied in chromium (VI) separation from aqueous solutions, *J. Hazard. Mater.*, 197 (2011) 244–253.
- [8] M. Ulewicz, E. Radzimska-Lenarcik, Application of polymer inclusion membranes doped with 1-hexyl-4-methylimidazole for pertraction of zinc(II) and other transition metal ions, *Physicochem. Prob. Miner. Process.*, 51 (2015) 447–460.
- [9] A. Garcia-Rodríguez, V. Matamoros, S.D. Kolev, C. Fontàs, Development of a polymer inclusion membrane (PIM) for the preconcentration of antibiotics in environmental water samples, *J. Membr. Sci.*, 492 (2015) 32–39.
- [10] N. Bayou, O. Arous, M. Amara, H. Kerdjoudj, Elaboration and characterization of a plasticized cellulose triacetate membrane containing trioctylphosphine oxide (TOPO): application to the transport of uranium and molybdenum ions, *C.R. Chim.*, 13 (2010) 1370–1376.
- [11] Y. Yildiz, A. Manzak, B. Aydın, O. Tutkun, Preparation and application of polymer inclusion membranes (PIMs) including alamine 336 for the extraction of metals from an aqueous solution, *Adv. Mater. Res.*, 48 (2014) 791–796.
- [12] G. Salazar-Alvarez, A.-N. Bautista-Flores, E. Rodriguez de San Miguel, M. Muhammeda, J. Gyves, Transport characterisation of a PIM system used for the extraction of Pb(II) using D2EHPA as carrier, *J. Membr. Sci.*, 250 (2005) 247–257.
- [13] N. Kavitha, K. Palanivelu, Recovery of copper(II) through polymer inclusion membrane with di(2-ethylhexyl) phosphoric

- acid as carrier from e-waste, *J. Membr. Sci.*, 415–416 (2012) 663–669.
- [14] P.R. Danesi, L. Reichley-Yinger, P.G. Rickert, Lifetime of supported liquid membranes: the influence of interfacial properties, chemical composition and water transport on the long-term stability of the membranes, *J. Membr. Sci.*, 31 (1987) 117–145.
- [15] M.-F. Paugam, J. Buf, Comparison of carrier-facilitated copper(II) ion transport mechanisms in a supported liquid membrane and in a plasticized cellulose triacetate membrane, *J. Membr. Sci.*, 147 (1998) 207–215.
- [16] G. Arthanareeswaran, P. Thanikaivelan, K. Srinivasan, D. Mohan, M. Rajendran, Synthesis, characterization and thermal studies on cellulose acetate membranes with additive, *Eur. Polym. J.*, 40 (2004) 2153–2159.
- [17] J.S. Gardner, J.S. Gardner, J.O. Walker, J.D. Lamb, Permeability and durability effects of cellulose polymer variation in polymer inclusion membranes, *J. Membr. Sci.*, 229 (2004) 87–93.
- [18] L.-A. Manjarrez Nevárez, L.-B. Casarrubias, A. Celzard, V. Fierro, V.-T. Muñoz, A.-C. Davila, J.-R. Torres Lubian, G.-G. Sánchez, Biopolymer-based nanocomposites: effect of lignin acetylation in cellulose triacetate films, *Sci. Technol. Adv. Mater.*, 12 (2011) 045006.
- [19] R.-L. Wu, X.-L. Wanga, F. Li, H.-Z. Li, Y.-Z. Wanga, Green composite films prepared from cellulose, starch and lignin in room-temperature ionic liquid, *Bioresour. Technol.*, 100 (2009) 2569–2574.
- [20] Y. Habibi, W.-K. El-Zawawy, M.-M. Ibrahim, A. Dufresne, Processing and characterization of reinforced polyethylene composites made with lignocellulosic fibers from Egyptian agro-industrial residues, *Compos. Sci. Technol.*, 68 (2008) 1877–1885.
- [21] A.-V. Maldhure, A.-R. Chaudhari, J.-D. Ekhe, Thermal and structural studies of polypropylene blended with esterified industrial waste lignin, *J. Therm. Anal. Calorim.*, 103 (2011) 625–632.
- [22] S. Laurichesse, L. Avérous, Chemical modification of lignins: towards biobased polymers, *Prog. Polym. Sci.*, 39 (2014) 1266–1290.
- [23] A. Gregorova, S. Redik, V. Sedlarik, F. Stelzer, Lignin-containing polyethylene films with antibacterial activity, *NANOCON, Proc. 3rd International Conference 21–23 September 2011, Brno Czech Republic*, Thomson Reuters, 2011.
- [24] L. Manjarrez Nevarez, L. Ballinas Casarrubias, O. Solis Canto, A. Celzard, V. Fierro, R. Ibarra Gomez, G. Gonzalez Sanchez, Biopolymers-based nanocomposites: membranes from propionated lignin and cellulose for water purification, *Carbohydr. Polym.*, 86 (2011) 732–741.
- [25] M. Inês, G.S. Almeida, R.W. Cattrall, S.D. Kolev, Recent trends in extraction and transport of metal ions using polymer inclusion membranes (PIMs), *J. Membr. Sci.*, 415–416 (2012) 9–23.
- [26] C.V. Gherasim, M. Cristea, C.V. Grigoras, G. Bourceanu, New polymer inclusion membrane: preparation and characterization, *Dig. J. Nanomater. Biostruct.*, 6 (2011) 1499–1508.
- [27] N. Cachet, S. Camy, B. Benjelloun-Mlayah, J.S. Condoret, M. Delmas, Esterification of organosolv lignin under supercritical conditions, *Ind. Crops Prod.*, 58 (2014) 287–297.
- [28] C. Fontàs, R. Tayeb, M. Dhahbi, E. Gaudichet, F. Thominet, P. Roy, K. Steenkeste, M.P. Fontaine-Aupart, S. Tingry, E. Tronel-Peyroz, P. Seta, Polymer inclusion membranes: the concept of fixed sites membrane revised, *J. Membr. Sci.*, 290 (2007) 62–72.
- [29] L.M. Kline, D.G. Hayes, A.R. Womac, N. Labbé, Simplified determination of lignin content in hard and soft woods via UV-spectrophotometric analysis of biomass dissolved in ionic liquids, *Bioresources*, 5 (2010) 1366–1383.
- [30] Y. Chen, N.-M. Stark, Z. Cai, C.-R. Frihart, L.-F. Lorenz, R.-E. Ibach, Chemical modification of kraft lignin: effect on chemical and thermal properties, *Bioresources*, 9 (2014) 5488–5500.
- [31] B. Xiao, X.-F. Sun, R. Sun, The chemical modification of lignins with succinic anhydride in aqueous systems, *Polym. Degrad. Stab.*, 71 (2001) 223–231.
- [32] N.-E. Elmansouri, Q. Yuan, F. Huang, Characterization of alkaline lignins for use in phenol-formaldehyde and epoxy resins, *Bioresources*, 6 (2011) 2647–2662.
- [33] A.R. Gonçalves, U. Schuchardt, M.L. Bianchi, A.A.S. Curvelo, Piassava fibers (*Attalea funifera*): NMR spectroscopy of their lignin, *J. Braz. Chem. Soc.*, 11 (2000) 491–494.
- [34] O. Gordobil, I. Egués, R. Llano-Ponte, J. Labidi, Physicochemical properties of PLA lignin blends, *Polym. Degrad. Stab.*, 108 (2014) 330–338.
- [35] V. Tserki, P. Matzinos, S. Kokkou, C. Panayiotou, Novel biodegradable composites based on treated lignocellulosic waste flour as filler. Part I. Surface chemical modification and characterization of waste flour, *Composites Part A*, 36 (2005) 965–974.
- [36] O. Arous, F.S. Saoud, M. Amara, H. Kerdjoudj, Efficient facilitated transport of lead and cadmium across a plasticized triacetate membrane mediated by D2EHPA and TOPO, *Mater. Sci. Appl.*, 2 (2011) 615–623.
- [37] O. Arous, H. Kerdjoudj, P. Seta, Comparison of carrier-facilitated silver (i) and copper (ii) ions transport mechanisms in a supported liquid membrane and in a plasticized cellulose triacetate membrane, *J. Membr. Sci.*, 241 (2004) 177–185.
- [38] O. Kebiche-Senhadj, S. Bey, G. Clarizia, L. Mansouri, M. Benamor, Gas permeation behavior of CTA polymer inclusion membrane (PIM) containing an acidic carrier for metal recovery (DEHPA), *Sep. Purif. Technol.*, 80 (2011) 38–44.
- [39] A. Tor, G. Arslan, H. Muslu, A. Celiktas, Y. Cengeloglu, M. Ersoz, Facilitated transport of Cr(III) through polymer inclusion membrane with di(2-ethylhexyl)phosphoric acid (DEHPA), *J. Membr. Sci.*, 329 (2009) 169–174.
- [40] G. Arslan, A. Tor, Y. Cengeloglu, M. Ersoz, Facilitated transport of Cr(III) through activated composite membrane containing di-(2-ethylhexyl)phosphoric acid (D2EHPA) as carrier agent, *J. Hazard. Mater.*, 165 (2009) 729–735.
- [41] H.D. Rozman, K.W. Tan, R.N. Kumar, A. Abubakar, Z.A. Mohd. Ishak, H. Ismail, The effect of lignin as a compatibilizer on the physical properties of coconut fiber-polypropylene composites, *Eur. Polym. J.*, 36 (2000) 483–494.
- [42] M.I. Vázquez, V. Romero, C. Fontàs, E. Anticó, J. Benavente, Polymer inclusion membranes (PIMs) with the ionic liquid (IL) Aliquat 336 as extractant: effect of base polymer and IL concentration on their physical-chemical and elastic characteristics, *J. Membr. Sci.*, 455 (2014) 312–319.
- [43] I. Marzouk, C. Hannachi, L. Dammak, B. Hamrouni, Removal of chromium by adsorption on activated alumina, *Desal. Wat. Treat.*, 26 (2011) 279–286.
- [44] M. Baczynska, M. Regel-Rosocka, M. Nowicki, M. Wisniewski, Effect of the structure of polymer inclusion membranes on Zn(II) transport from chloride aqueous solutions, *J. Appl. Polym. Sci.*, 132 (2015) 42319.
- [45] A. Zaghbani, R. Tayeb, M. Dhahbi, M. Hidalgo, F. Vocanson, I. Bonnamour, P. Seta, C. Fontàs, Selective thiocalix[4]arene bearing three amide groups as ionophore of binary Pd(II) and Au(III) extraction by a supported liquid membrane system, *Sep. Purif. Technol.*, 57 (2007) 374–379.
- [46] A. Gherrou, H. Kerdjoudj, R. Molinari, P. Seta, Preparation and characterization of polymeric plasticized membranes (PPM) embedding a crown ether carrier. Application to copper ions transport, *Mater. Sci. Eng., C*, 25 (2005) 436–443.
- [47] B. Pośpiech, W. Walkowiak, Separation of copper(II), cobalt(II) and nickel(II) from chloride solutions by polymer inclusion membranes, *Sep. Purif. Technol.*, 57 (2007) 461–465.
- [48] A. Casadellà, O. Schaetzle, K. Nijmeijer, K. Loos, Polymer inclusion membranes (PIM) for the recovery of potassium in the presence of competitive cations, *Polymers*, 8 (2016) 76.
- [49] O. Kebiche-Senhadj, L. Mansouri, S. Tingry, P. Seta, M. Benamor, Facilitated Cd(II) transport across CTA polymer inclusion membrane using anion (Aliquat 336) and cation (D2EHPA) metal carriers, *J. Membr. Sci.*, 310 (2008) 438–445.